

# Exploring Isovalent Substitution of Lead with Nickel in Methylammonium Lead Iodide Perovskites

*Emily C. Smith<sup>a</sup>, Hamza Javaid<sup>a</sup>, Muhammad Abdullah<sup>a</sup>, Kevin R. Kittilstved<sup>a\*</sup>, D.*

*Venkataraman<sup>a\*</sup>*

<sup>a</sup> Department of Chemistry, University of Massachusetts Amherst, Amherst Massachusetts 01003-9303, United States

## ABSTRACT

We replaced lead ions with nickel ions in methylammonium lead triiodide (MAPbI<sub>3</sub>) perovskites and studied their electronic and photophysical properties. We synthesized thin films using solutions containing methylammonium iodide (MAI), PbI<sub>2</sub>, and NiI<sub>2</sub> with varying Pb/Ni precursor ratios. We show that MAPbI<sub>3</sub> retains its three-dimensional perovskite structure in the presence of Ni<sup>2+</sup>. We were able to incorporate up to 30% Ni<sup>2+</sup> before we note the appearance of unconverted NiI<sub>2</sub> via X-ray diffraction. Although the structures of NiI<sub>2</sub> and PbI<sub>2</sub> are isostructural and the metal ions have the same oxidation states, the bulk material did not behave as a solid solution. Furthermore, the addition of Ni<sup>2+</sup> thoroughly quenched the emission of MAPbI<sub>3</sub>, suggesting that Ni<sup>2+</sup> may act as a recombination center for excited charge carriers. Additionally, the materials displayed significant instability towards water. Thus, we conclude that there is a limited application for nickel and perhaps other transition metal ions as a replacement ion for lead in thin-film perovskite photovoltaic devices fabricated in these conditions.

## INTRODUCTION

The environmental and toxicity concerns of lead in hybrid organic-inorganic perovskite (HOIP) solar may become a limiting factor in the large-scale and widespread deployment of these devices.<sup>1</sup> Thus, there are continuing efforts to replace  $\text{Pb}^{2+}$  with other ions in the crystalline structure while maintaining the optical and electronic properties. The most obvious choices to replace  $\text{Pb}^{2+}$  are the group 14 ions such as  $\text{Sn}^{2+}$  and  $\text{Ge}^{2+}$ , which have been extensively studied.<sup>2,3</sup> However, thus far, these ions have been met with limited success in part due to their instability to oxidation. Therefore, we need to need explore other alternatives.<sup>1,4</sup> A number of transition metal ions are of particular interest in the replacement of  $\text{Pb}^{2+}$  due to their rich oxidation chemistry, low toxicity, and relative abundance.<sup>3,5</sup> In fact, computational screening studies predict that HOIPs containing metal ions such as  $\text{Mg}^{2+}$ ,  $\text{V}^{2+}$ ,  $\text{Mn}^{2+}$ , and  $\text{Ni}^{2+}$  are likely to function as direct bandgap semiconductors and are good candidates for replacing  $\text{Pb}^{2+}$  ions.<sup>6</sup> However these predictions have not been experimentally verified. Herein, we study the optical and structural properties of methylammonium lead triiodide ( $\text{MAPbI}_3$ ) films with varying degrees of  $\text{Ni}^{2+}$  substitution. We show that the three-dimensional (3D) perovskite structure is maintained with increasing ratios of  $\text{NiI}_2$  of up to 30%  $\text{Ni}^{2+}$ . Interestingly, we observed that the mixing of  $\text{NiI}_2$  and  $\text{PbI}_2$  precursors did not produce uniformly mixed films in the solid-state, as analyzed by X-ray diffraction and visible absorption studies. We report optical bandgaps for the  $\text{Ni}^{2+}$  substituted films between 1.3 and 1.6 eV, which appear to be independent of the  $\text{Ni}^{2+}$  concentration. Furthermore, we observe quenching of emission from  $\text{MAPbI}_3$  upon  $\text{Ni}^{2+}$  substitution, indicating the  $\text{Ni}^{2+}$  may act as a recombination center for charge carriers. Lastly, the  $\text{Ni}^{2+}$  substituted films displayed high sensitivity to water, as observed by rapid color changes of the films on exposure to ambient conditions. Thus, despite the optimal bandgap and structure of the materials, we

conclude that  $\text{Ni}^{2+}$  is not a promising candidate for  $\text{Pb}^{2+}$  replacement in these conditions (e.g. polycrystalline thin-films deposited from  $\text{NiI}_2$  precursors) for HOIP solar cells.

## EXPERIMENTAL METHODS

**Precursor Solutions.** In a nitrogen-filled glove box, methylammonium iodide (158 mg, 1 mmol) and  $\text{PbI}_2$  (461 mg, 1 mmol) were added to a vial followed by 1 mL of a co-solvent containing anhydrous dimethylformamide (DMF) and dimethylsulfoxide (DMSO) (v:v 8:2). For mixtures of ions, up to 0.5 mmol  $\text{NiI}_2$  (50%  $\text{Ni}^{2+}$ ) was added to the  $\text{PbI}_2$  solution in various ratios while maintaining the total metal halide salt content at 1 mmol. For example, the 30%  $\text{Ni}^{2+}$  mixture was prepared by adding 0.7 mmol of  $\text{PbI}_2$  and 0.3 mmol of  $\text{NiI}_2$  to total 1 mmol. We also experimented with 2-fold decrease in precursor concentrations (0.5 mmol MAI and 0.5 mmol  $\text{NiI}_2/\text{PbI}_2$ ), and we observed similar structure and optical properties in these films. The solutions were prepared based on the procedure reported by Siegler et.al.<sup>7,8</sup> The solutions were stirred on a hot plate at 110 °C for 2 h. DMSO solutions containing  $\text{NiI}_2$  appeared light green in color, consistent with solvated  $\text{Ni}^{2+}$  ions. The solutions were kept hot until just before film preparation, since removing them from the heat-induced precipitation of the  $\text{NiI}_2$  salt. Solutions were prepared directly before spin coating, as old solutions appeared to degrade over time resulting in X-ray diffraction patterns with impurity phases.

**Hybrid Organic Inorganic Perovskite Films.** Glass substrates (1 mm × 1 mm) were washed by sonicating in a soap and water bath, then with water, acetone, and isopropyl alcohol for 20 min each. The substrates were dried in an oven and 140 °C for at least 1 h. Hot precursor solutions were spin cast onto the substrates in non-ambient conditions (50  $\mu\text{L}$  at 3000 rpm for 30 s). The films were then annealed at 110 °C for 5-25 min. Longer annealing times led to increase in the

intensity of the peaks associated with  $\text{PbI}_2$  as observed by powder X-ray diffraction. For X-ray diffraction, the films were encapsulated in a mylar plastic sample holder. For optical studies, the films were encapsulated in between 2 pieces of transparent packing tape to protect the samples from exposure to ambient water. The films appeared to rapidly degrade upon exposure to ambient conditions (within a matter of minutes) as noted by a color change from black to light brown/clear. No immediate color change was noted for encapsulated films upon exposure of ambient conditions. However, to prevent water exposure, the films were only removed from non-ambient conditions for testing and were returned to the dry environment upon completion.

***Physical Characterization.*** Absorption studies were carried out on an Agilent Cary 50 Bio spectrophotometer. Films were measured in transmission mode from 300 – 900 nm. The optical bandgap was estimated from Tauc plots analysis and assumed a direct, allowed transition. Emission studies were carried out on an Agilent Cary Eclipse Fluorescence spectrophotometer. Films were excited at  $\lambda_{\text{ex}} = 450$  nm and measured from 700 – 850 nm. Powder X-Ray diffraction (XRD) was taken in a Bragg-Brentano configuration using a Rigaku SmartLab SE X-ray diffractometer with a D/tex 250 Ultra ID Si strip detector. Measurements were taken from  $2\theta = 10^\circ$  to  $50^\circ$  with a  $\text{Cu K}\alpha$  (1.542 Å) X-ray source.

## RESULTS AND DISCUSSION

We prepared films with varying degrees of nominal  $\text{Ni}^{2+}$  mol fraction ranging from 0-50%  $\text{Ni}^{2+}$ . All films with  $\text{Ni}^{2+}$  content between 0% and 50% showed evidence of 3D perovskite in the

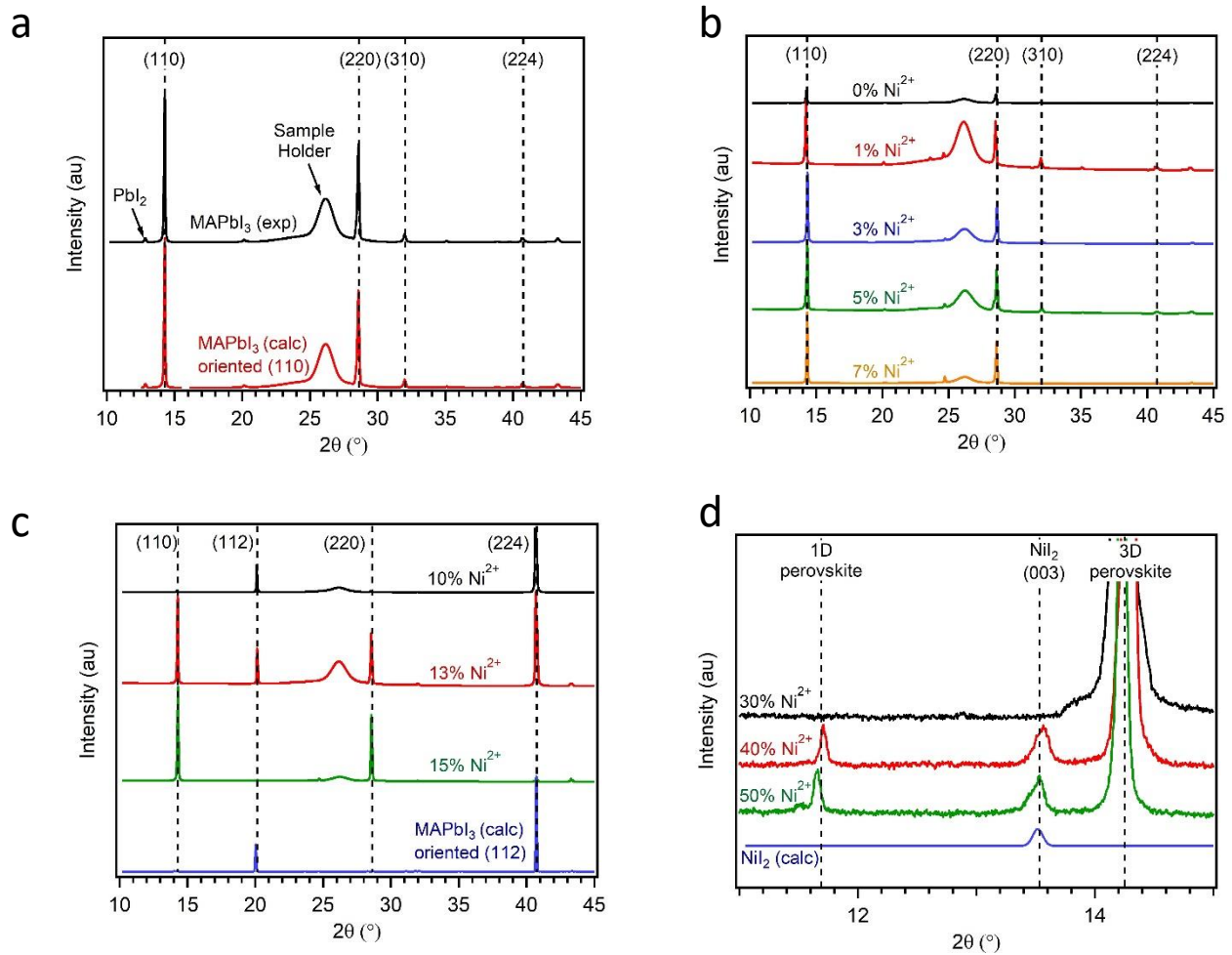


**Figure 1.** Powder X-ray diffraction patterns of: a) Experimental MAPbI<sub>3</sub> (black) and MAPbI<sub>3</sub> with calculated partial orientation along the (110) plane (from ref. 9) b) patterns for films ranging from 0 – 7% Ni<sup>2+</sup> substitution which show that the partial orientation along (110) is maintained c) films ranging from 10 – 15% Ni<sup>2+</sup> substitution showing an orientational shift along the (112) plane and MAPbI<sub>3</sub> with calculated orientation along the (112) plane (from ref. 9) d) films ranging from 30 – 50% Ni<sup>2+</sup> showing the emergence of unconverted NiI<sub>2</sub> peaks, and calculated NiI<sub>2</sub> pattern.

tetragonal phase,<sup>9</sup> as seen in the powder X-ray diffraction patterns (Figure 1). We observed a broad, amorphous peak in all samples between 21° – 27° 2θ resulting from the air-free mylar sample holder. Upon addition of ≥40% Ni<sup>2+</sup>, we observe a new peak at 13.5° 2θ, which corresponds to the (330) plane of NiI<sub>2</sub> present as a secondary phase (Figure 1d). This peak shifts to lower 2θ values upon the incorporation of 50% Ni<sup>2+</sup> may arise due to the poor signal-to-noise of this peak. Films containing ≥40% Ni<sup>2+</sup> displays an additional peak at ~11° 2θ, which is typically attributed to lower dimensional perovskite (1D) phases.<sup>10,11</sup> Thus, we conclude that the upper limit of Ni<sup>2+</sup>

incorporation into the 3D perovskite structure under these conditions is 30%. We note that  $\text{NiI}_2$  solubility in the precursor solution was relatively low, even at high temperatures. We hypothesize that the 40% and 50%  $\text{Ni}^{2+}$  concentrations likely exceed the solid solubility limit of  $\text{Ni}^{2+}$  substitution in the  $\text{MAPbI}_3$  films, thus resulting in the formation of  $\text{NiI}_2$ .

In pristine  $\text{MAPbI}_3$  film (0%  $\text{Ni}^{2+}$ ), we observed a small peak at  $12.5^\circ 2\theta$  corresponding to  $\text{PbI}_2$ . We attribute sample degradation to the high annealing temperature. As expected, annealing at this temperature for a longer time (25 min) results in an increased relative intensity of  $\text{PbI}_2$ -related peaks. Additionally, pristine  $\text{MAPbI}_3$  films display preferred orientation along the (110) plane (Figure 1a).<sup>9</sup> This orientation is preserved with nominal  $\text{Ni}^{2+}$  concentrations up to 7% (Figure 1b). Interestingly, upon addition of 10 %  $\text{Ni}^{2+}$ , there is a reorientation of the films along the (112) plane (Figure 1c). However, despite the orientational change, the patterns clearly show that the 3D perovskite structure is maintained in these films. We initially hypothesized that this result could be due to the insolubility of the precursor  $\text{NiI}_2$  at these concentrations, causing it to precipitate more quickly onto the substrate resulting in new orientation of the films. However, when we increase the concentration of  $\text{Ni}^{2+}$  further (13 – 15 %  $\text{Ni}^{2+}$ ), we note that the orientation of the films reverts back to (110) as observed in the lower concentrated samples (Figure 1c). Therefore, we rule out the possibility that this response is due entirely to the solubility of  $\text{NiI}_2$  under these conditions. This behavior likely indicates that there is a secondary factor playing a role during the crystallization of these materials. The cause and nature of this response remains unknown.

To determine if these films behave as a solid solution, i.e.,  $\text{Ni}^{2+}$  and  $\text{Pb}^{2+}$  mix uniformly and randomly, we evaluated the d-spacing of the (110) peak as a function of  $\text{Ni}^{2+}$  concentration (Figure 2). Since  $\text{Ni}^{2+}$  (70 ppm) is a smaller ion than  $\text{Pb}^{2+}$  (119 ppm), we expect the d-spacing to decrease

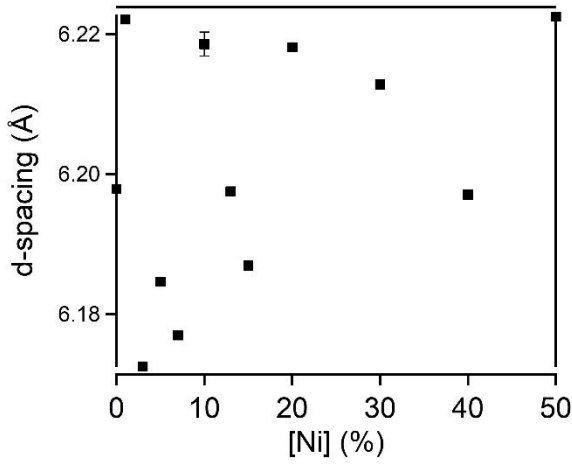


**Figure 2.** Calculated d-spacing from the (110) diffraction peak at  $\sim 14.3^\circ 2\theta$  for films with variable  $\text{Ni}^{2+}$  substitution. The lattice parameters do not shift to smaller d-spacings with a linear correlation as expected for uniform mixing of ions.

with increasing incorporation of  $\text{Ni}^{2+}$  corresponding to a shrinking lattice size. Furthermore, we expect a strong linear correlation between the unit cell parameters and  $\text{Ni}^{2+}$  ion concentration for a material with uniform mixing of the two metal ions. Interestingly, we did not observe any linear correlation between these two factors, nor did we observe a reduction in the d-spacing.

From this result we conclude that  $\text{Ni}^{2+}$  and  $\text{Pb}^{2+}$  mixtures do not mix uniformly at the nominal concentrations that we prepared. This may indicate that  $\text{Ni}^{2+}$  is not incorporated into the 3D structure. However, lack of diffraction peaks corresponding to unconverted  $\text{NiI}_2$  and low dimensional perovskite, as well as the orientational influence of  $\text{Ni}^{2+}$  in these compositions, suggests that it does influence the overall structure of the bulk material. Another possibility is that  $\text{Ni}^{2+}$  is not incorporated into the B site of the  $\text{ABX}_3$  perovskite structure when high nominal doping

concentrations are used. For example, is possible that  $\text{Ni}^{2+}$  could be excluded to grain boundaries, form secondary phases, or could create halide anti-site defects.

To evaluate the optical properties of the films, we conducted absorption and emission experiments at room temperature. The absorption and emission spectra of pristine  $\text{MAPbI}_3$  (0%  $\text{Ni}^{2+}$ ) are shown in Figure 3a. We observe an optical bandgap for  $\text{MAPbI}_3$  at approximately 1.4 eV (Figure 4) and emission at 1.6 eV (773 nm). The optical bandgaps

of samples containing  $\text{Ni}^{2+}$  range from 1.3 – 1.6 eV (Figure 4b), extrapolated from a Tauc plot (Figure 4a).<sup>12</sup> We note that the observed band gaps appear to be independent of  $\text{Ni}^{2+}$  concentration, which is another indicator that the  $\text{Ni}^{2+}$  may not be incorporating into the B site of the material, since the band edge is primarily derived from the metal and halide orbitals of the  $\text{BX}_6$  octahedra.<sup>13</sup>

In the visible region, the incorporation of  $\text{Ni}^{2+}$  produces two broad absorption features between 3.0 – 3.75 eV, which are not observed in pristine  $\text{MAPbI}_3$  (Figure 3b). Interestingly, the increased absorption coefficients in the visible range would be favorable for a solar cell device. However,

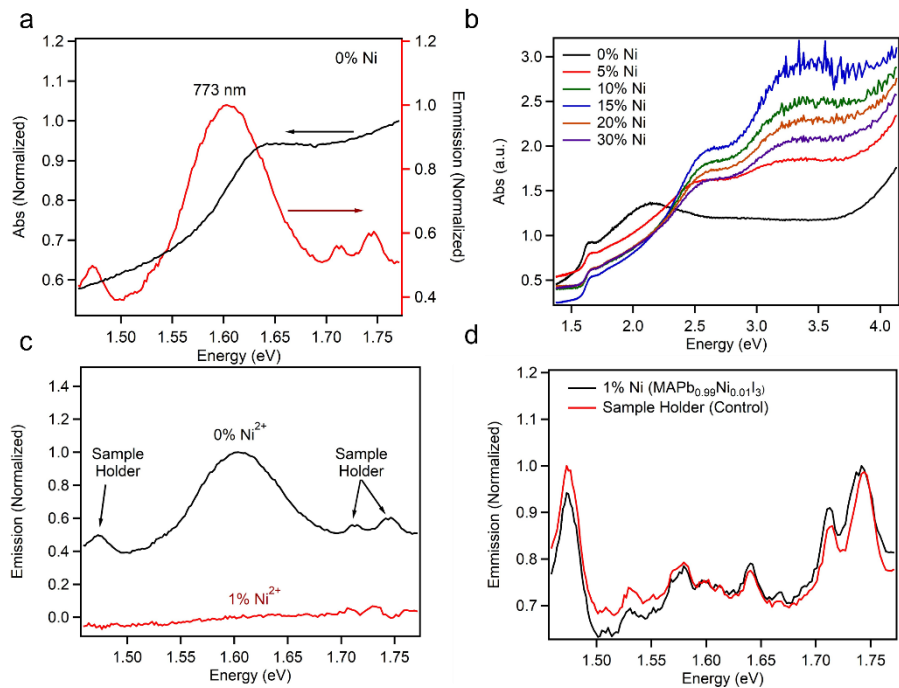


**Figure 1.** a) Absorption (black) taken in transmission mode and emission (red) of pristine  $\text{MAPbI}_3$  b) full absorption spectra for varying concentrations of  $\text{Ni}^{2+}$  showing new absorption features between 3.0 – 3.75 eV. The spectra tail upwards below 3.75 eV due to absorption from the sample holder. c) Normalized emission from 0%  $\text{Ni}^{2+}$  (black) and 1%  $\text{Ni}^{2+}$  (red, background subtracted) showing a broad emission at 1.6 eV (773 nm) that is quenched on the addition of  $\text{Ni}^{2+}$ . The small emission peaks at 1.5 and 1.7 eV result from the sample holder. d) Normalized emission of 1%  $\text{Ni}^{2+}$  compared to the sample holder showing no new emission features appear upon the addition of  $\text{Ni}^{2+}$ .



we also report strong emission quenching in these samples with the addition of any amount of  $\text{Ni}^{2+}$  (Figure 3c). We hypothesize that  $\text{Ni}^{2+}$  may act as a recombination center in devices due to the

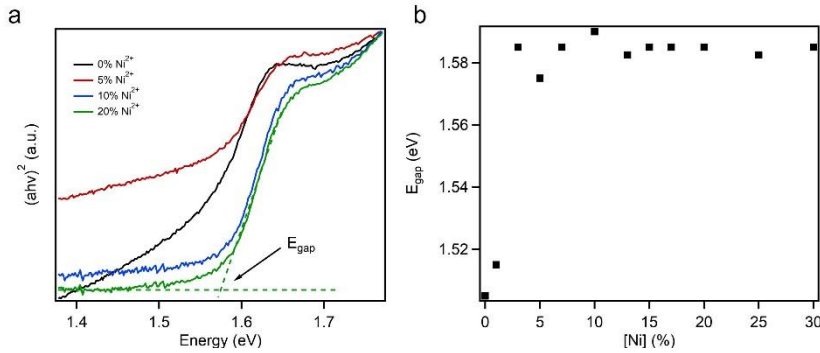


**Figure 2.** a) Tauc plots for some of the  $\text{Ni}^{2+}$  concentrations. The intersection between linear regions was determined to be the bandgap b) Optical band gaps derived from Tauc plots of films containing 0 – 30%  $\text{Ni}^{2+}$ .

presence of low-lying ligand field states that introduce non-radiative recombination pathways for the excitonic excited state. The lowest lying ligand field state in  $\text{NiI}_2$

single crystals occurs in the near-IR region at  $\sim 0.9$  eV, which supports the hypothesis that lower lying orbitals in Ni could provide sub gap states.<sup>14</sup> This observation is additionally consistent with theoretical calculations for  $\text{MA}(\text{Pb}_{1-x}\text{Ni}_x\text{Br}_3)$  which show that partial  $\text{Ni}^{2+}$  substitution leads to new mid-gap states.<sup>15</sup> Reported  $\text{MAPbI}_3$  solar cell devices doped with 10%  $\text{Ni}^{2+}$  show a significant reduction in current density, which is consistent with trap states inducing non-radiative recombination of charge carriers.<sup>16</sup> These results are not consistent with what has been observed for systems with 3%  $\text{Ni}^{2+}$  substitution, which shows that emission is retained in these systems.<sup>17</sup> In the present work, our films were encapsulated in a layer of clear plastic tape for the emission measurements. This encapsulation most likely significantly reduces the light power input and emission from the films, as indicated by the relatively low emission intensity of the control sample (0%  $\text{Ni}^{2+}$ ). Therefore, the complete quenching effect we observe in even the lowest concentration (1%  $\text{Ni}^{2+}$ ) samples is most likely an overestimation of the actual quenching capability of  $\text{Ni}^{2+}$  in this system. Additionally, these materials displayed significant moisture sensitivity, with color changes from black to light brown/clear in a matter of seconds on exposure to moisture. Given

this, we speculate that these materials are highly sensitive to changes in sample preparation and relative measurement conditions.

## CONCLUSION

We show that partial substitution of up to 30%  $\text{Ni}^{2+}$  into  $\text{MAPbI}_3$  thin films is possible while retaining the 3D perovskite structure.  $\text{Ni}^{2+}$  concentrations above 30% result in new low dimensional perovskite phases and unconverted  $\text{NiI}_2$  precursor. We do not observe correlations between unit cell parameters and  $\text{Ni}^{2+}$  concentration, which suggests that  $\text{Ni}^{2+}$  does not mix uniformly and may not substitute into the B site of the  $\text{ABX}_3$  perovskite as anticipated. The bandgap of the mixed materials ranges from 1.3 – 1.6 eV and is enhanced in the visible region with the incorporation of  $\text{Ni}^{2+}$ , which is optimal for a solar cell device. However, emission quenching suggests that  $\text{Ni}^{2+}$  may introduce new low-lying states that act as charge carrier traps which would limit device performance. Additionally, the significant water sensitivity of the materials limits the potential application of these materials in solar cells. Thus, we conclude that given the conditions presented in this paper,  $\text{Ni}^{2+}$  is not a good candidate for  $\text{Pb}^{2+}$  replacement in thin-film  $\text{MAPbI}_3$  solar cells prepared under these conditions.

## ACKNOWLEDGMENT

We gratefully acknowledge the financial support of US Army CCDC Soldier Center through contract no. W911QY1820002 for this work. We gratefully acknowledge the work of Samuel Stroup for help with some data acquisition. We thank Anand Ode and Kaleigh Ryan who were responsible for early studies which led to the conception of this research, and funding from the NSF REU program (CHE-1659266). The acquisition of the powder X-ray diffractometer was made

possible through the National Science Foundation Major Research Instrumentation Program (CHE-1726578).

### **Corresponding Authors**

D. Venkataraman – Department of Chemistry, University of Massachusetts Amherst, Amherst, MA 01003; <https://orcid.org/0000-0003-2906-0579>; Email: [dv@umass.edu](mailto:dv@umass.edu)

Kevin Kittilstved – Department of Chemistry, University of Massachusetts Amherst, Amherst, MA 01003; <https://orcid.org/0000-0002-9852-7454>; Email: [kittilstved@chem.umass.edu](mailto:kittilstved@chem.umass.edu)

### **Authors**

Emily C. Smith – Department of Chemistry, University of Massachusetts Amherst, Amherst, MA 01003; <https://orcid.org/0000-0002-0849-897X>

Hamza Javaid – Department of Chemistry, University of Massachusetts Amherst, Amherst, MA 01003

Muhammad Abdullah – Department of Chemistry, University of Massachusetts Amherst, Amherst, MA 01003

### **REFERENCES**

- 1 Ke, W. J. & Kanatzidis, M. G. Prospects for low-toxicity lead-free perovskite solar cells. *Nat. Commun.* **10**, 965, (2019), doi:10.1038/s41467-019-08918-3.
- 2 Konstantakou, M. & Stergiopoulos, T. A critical review on tin halide perovskite solar cells. *J. Mater. Chem. A* **5**, 11518-11549, (2017), doi:10.1039/c7ta00929a.

- 3     Hoefler, S. F., Trimmel, G. & Rath, T. Progress on lead-free metal halide perovskites for photovoltaic applications: a review. *Monatsh. Chem.* **148**, 795-826, (2017), doi:10.1007/s00706-017-1933-9.
- 4     Shi, Z. J. *et al.* Lead-Free Organic-Inorganic Hybrid Perovskites for Photovoltaic Applications: Recent Advances and Perspectives. *Adv. Mater.* **29**, 1605005, (2017), doi:10.1002/adma.201605005.
- 5     Chatterjee, S. & Pal, A. J. Influence of metal substitution on hybrid halide perovskites: towards lead-free perovskite solar cells. *J. Mater. Chem. A* **6**, 3793-3823, (2018), doi:10.1039/c7ta09943f.
- 6     Filip, M. R. & Giustino, F. Computational Screening of Homovalent Lead Substitution in Organic-Inorganic Halide Perovskites. *J. Phys. Chem. C* **120**, 166-173, (2016), doi:10.1021/acs.jpcc.5b11845.
- 7     Siegler, T. D. *et al.* Deliquescent Chromism of Nickel(II) Iodide Thin Films. *Langmuir* **35**, 2146-2152, (2019), doi:10.1021/acs.langmuir.8b03979.
- 8     Raw, A. D., Ibers, J. A. & Poeppelmeier, K. R. Syntheses and structure of hydrothermally prepared CsNiX<sub>3</sub> (X=Cl, Br, I). *J. Solid State Chem.* **192**, 34-37, (2012), doi:10.1016/j.jssc.2012.03.037.
- 9     Szafranski, M. & Katrusiak, A. Mechanism of Pressure-Induced Phase Transitions, Amorphization, and Absorption-Edge Shift in Photovoltaic Methylammonium Lead Iodide. *J. Phys. Chem. Lett.* **7**, 3458-3466, (2016), doi:10.1021/acs.jpclett.6b01648.
- 10    Seth, C. & Khushalani, D. Non-Perovskite Hybrid Material, Imidazolium Lead Iodide, with Enhanced Stability. *ChemNanoMat* **5**, 85-91, (2019), doi:10.1002/cnma.201800375.

- 11 Mancini, A. *et al.* Synthesis, structural and optical characterization of APbX<sub>3</sub> (A=methylammonium, dimethylammonium, trimethylammonium; X=I, Br, Cl) hybrid organic-inorganic materials. *J. Solid State Chem.* **240**, 55-60, (2016), doi:10.1016/j.jssc.2016.05.015.
- 12 Viezbicke, B. D., Patel, S., Davis, B. E. & Birnie, D. P. Evaluation of the Tauc method for optical absorption edge determination: ZnO thin films as a model system. *Phys. Status Solidi B-Basic Solid State Phys.* **252**, 1700-1710, (2015), doi:10.1002/pssb.201552007.
- 13 Yin, W. J., Shi, T. T. & Yan, Y. F. Unique Properties of Halide Perovskites as Possible Origins of the Superior Solar Cell Performance. *Adv. Mater.* **26**, 4653-4658, (2014), doi:10.1002/adma.201306281.
- 14 Rosseinsky, D. R. & Dorrity, I. A. Absorption spectrum of single crystals of nickel iodide at 300-5 K. *Inorganic Chemistry* **17**, 1600-1603, (1978), doi:10.1021/ic50184a041.
- 15 Mannodi-Kanakkithodi, A. *et al.* Comprehensive Computational Study of Partial Lead Substitution in Methylammonium Lead Bromide. *Chemistry of Materials*. **31**, 3599-3612, (2019), doi:10.1021/acs.chemmater.8b04017.
- 16 Frolova, L. A., Anokhin, D. V., Gerasimov, K. L., Dremova, N. N. & Troshin, P. A. Exploring the Effects of the Pb<sup>2+</sup> Substitution in MAPbI<sub>3</sub> on the Photovoltaic Performance of the Hybrid Perovskite Solar Cells. *J. Phys. Chem. Lett.* **7**, 4353-4357, (2016), doi:10.1021/acs.jpcclett.6b02122.
- 17 Zheng, H. Y. *et al.* Acquiring High-Performance and Stable Mixed-Dimensional Perovskite Solar Cells by Using a Transition-Metal-Substituted Pb Precursor. *ChemSusChem* **11**, 3269-3275, (2018), doi:10.1002/cssc.201801171.